

## Three-Dimensional Microscopy of Surfaces by Grazing Incidence Diffraction

This paper discloses a novel technology for metrological 3D microscopy. Unlike conventional microscopy where field-of-view is constrained by depth resolution or touch probes which are limited to a single point, this method exploits an anamorphic leverage unique to diffraction and is based on holographically fabricated primary objectives. This type of 3D inspection microscope can accommodate lateral line widths that are many times wider than their corresponding depth window. The method preserves depth-of-field and has an order-of-magnitude improvement in stand-off compared with conventional refraction microscopy.

Industrial process and quality control inspection microscopy has always been hampered by a narrow field-of-view and limited stand-off. These problems, bad enough in conventional 2D microscopy, are aggravated when acquiring the third dimension. 3D triangulation sensors offer fractional lateral field to depth ratios, and confocal microscopy is a point-by-point method with a very limited stand-off. Touch probe CMM's and related contact mechanical instruments such as micrometers are accurate but tedious with no stand-off. These problems affect surface inspection metrology where circuit boards, web processed fibers, and conveyor belt manufacturing processes present wide targets with surface anomalies that must be quantified to micron accuracy by non-contact instruments. We offer a novel solution to long-standing problems in industrial inspection with additional applications in motion control for micro robotics, medicine, biology, archeology, and other sciences requiring 3D microscopy.

### Background

The anamorphic magnification we exploit could not be observed until high frequency gratings became available in the twentieth century. Even with fine pitch plane gratings, anamorphic ratio was limited at 2:1, similar to cylindrical lenses. To achieve higher ratios of anamorphic magnification, holography had to be invented. The original application of holography proposed by Gabor in 1948 was for a process that would improve electron microscopy.<sup>1</sup> Gabor's theory of wave front reconstruction, as applied to magnification, proved impractical as he described it, and holographic microscopy was never fully realized.<sup>2</sup>

In 1987 Tom DeWitt (now surnamed Ditto) received a patent that was based on the observation that higher-order diffraction images scale as a function of the distance of a source of illumination from a diffraction grating.<sup>3</sup> This simple ranging method could not be found in the literature, and the patent was awarded without an Office Action in the U.S. and then went on to stand in Europe and Japan, as well.<sup>4</sup>

While implementing a novel 3D ranging method under an NSF Phase II SBIR<sup>5</sup> in 1995, we predicted that the excursion of the higher-order image could be controlled with variable pitch gratings. A silver halide holographic grating was fabricated in a manner that would reconstruct wavefronts inside a selected working volume according to a prescription for linearity. The hologram was used as the primary objective in a profilometer. When a projected sheet of light was used to interrogate the working volume, the camera recorded 3D surface profiles without perspective foreshortening. The method has been shown to overcome near-field blindness and perspective foreshortening endemic to almost all triangulation 3D profilometry systems. The prototype of a hand held scanner based on the method was named SBIR Sensor and Instrumentation of the Year prize by a NASA-staffed jury in 1997.<sup>6</sup> A peer-reviewed disclosure was published in *Optical Engineering* in 2000.<sup>7</sup> A patent for the method issued in the US in December 2002<sup>8</sup> and in 2003 the patent issued in Europe through the EPO.<sup>9</sup> The patent is under Examination in Canada<sup>10</sup> and has been filed in Japan.<sup>11</sup>

### Principle

An investigation of diffraction range finding by Ditto revealed magnification features that can be achieved using gratings in grazing incidence or grazing exodus configurations. When configured at grazing exodus, a grating can be used in a telescope.<sup>12</sup> However, when incident wavefronts are reconstructed at grazing incidence angles, the optics exhibit leverage suitable for resolving microscopic dimensions.<sup>13</sup>

The geometry of grazing incidence in a diffraction range finder exhibits an intrinsic anamorphic magnification. A narrow waist of input rays is expanded to the full width of the grating itself. The anamorphic magnification is the ratio of the length of the grating to the waist of the input. See Figure 1.

Anamorphic magnification is a topic in teaching diffraction grating optics.<sup>14</sup> However, the utility of diffraction grating magnification in a microscope has not been exploited, notwithstanding that the raw numbers suggest that the phenomenon has an application in 3D microscopy. As the input angle approaches grazing incidence, the ratio of the grating length to the input waist expands exponentially reaching a limit imposed by the wavelength of the incident radiation.

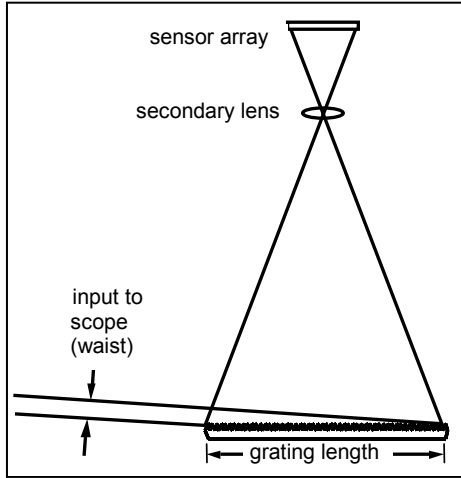


Fig 1 Anamorphic grating magnification

Surface relief types of diffraction gratings readily lend themselves to the grazing incidence configuration. Wavefront reconstruction at a grazing angle proceeds as it does at any other angle. Flux extinction can occur at angles of diffraction approaching evanescence ( $i = 90^\circ$ ) when surface peaks block radiation originating in troughs, but flatness tolerances for serviceable image acuity at visible wavelengths are inside the flatness specifications of garden-variety optical flats.<sup>15</sup> Grazing incidence plane gratings have become part of commercial lines<sup>16</sup> and are routinely used for varying laser wavelength through a feedback regime.<sup>17</sup>

In order for periodic waves to be directed from a flat grating to a focal point, the specification for groove spacing must be of variable pitch (also called *chirped* frequency). Such gratings can be manufactured holographically by duplicating the ray paths desired on playback. The fundamental type of hologram is fabricated by the intersection of a plane wave referenced by a spherical wave. At any wave length of incident radiation  $\lambda$ , the pitch  $p$  of the resulting grating can be known from the angles of incident radiation  $i$  and reconstruction  $r$ . For grazing angles, the diffraction order can be restricted to either  $n = 1$  or  $n = -1$ .

$$(1) \quad p = \frac{n\lambda}{\sin(i) - \sin(r)}$$

In the case of a hologram where the incident angle  $i$  is a constant established by a plane wave and the angle of reconstruction  $r$  varies continuously inside a cone of light according to the angle determined by a spherical wave, this relationship for pitch yields a parabolic variation in grating groove pitch along the axis of the incident illumination.

We diagram the relevant parameters in Figure 2.

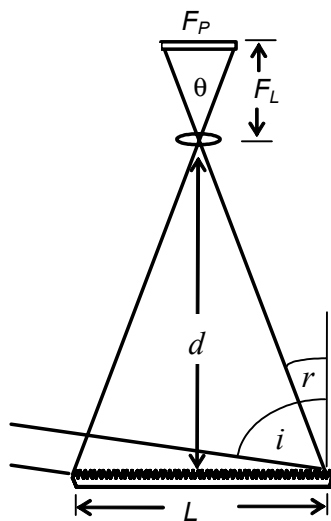


Figure 2 Parameterization of model

We are interested in grazing angles, subtending  $i > 80^\circ$ . The reconstruction angles vary, but we know that the greatest magnification will occur when light is collected at a point of  $r = 0^\circ$ , because it is along this axis that the secondary objective will have its widest field-of-view  $\theta$ .

$$(2) \quad \theta = 2 \arctan\left(\frac{L}{2d}\right)$$

For a given focal plane width  $F_p$  there will be a focal length  $F_L$  for the secondary objective such that a grating of given length will fill the field-of-view.

$$(3) \quad F_L = \frac{F_p}{2 \tan\left(\frac{\theta}{2}\right)}$$

The grating period can be modeled for reconstruction by a specified secondary objective lens and a focal plane array of known length. In equation (4), below, we say

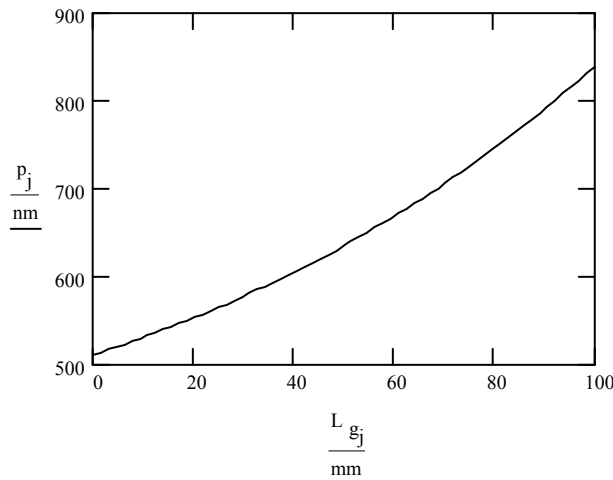


Figure 3 Grating pitch vs grating length

interrogation beam as known from the angle  $r$  of reconstruction.

$$(5) \quad D_L = \frac{\kappa(d \tan(r) - s)}{\cos(\alpha) - \kappa \sin(\alpha)}$$

where

$$(6) \quad \kappa = \frac{\sqrt{1 - \left(n \frac{\lambda}{p} + \sin(r)\right)^2}}{n \frac{\lambda}{p} + \sin(r)}$$

and

$$(7) \quad s = \frac{L}{2}$$

Occlusion liability is determined by subtracting the laser angle from the incident angle

$$(8) \quad \beta = i - \alpha$$

Consider the grating pitches graphed in Figure 3 where the angle of grazing incidence is 88 degrees, and the secondary lens is 200 mm from a 100 x 100 mm grating. Using equations 5-8 we generate a graph of Figure 4 showing the range along the laser line  $D_L$  vs. focal plane displacement  $x$  where the camera focal plane is 6.4 mm wide (+/- 3.2mm around the origin 0). We have selected three entry angles  $\alpha$  for the interrogating laser: 0, 40 and 80 degrees. There is a tradeoff between depth and occlusion liability. In the case where occlusion liability is less than 10 degrees, range window is 15 mm. Using a camera with 1,500 photo sites, the nominal resolution would be 1 micron. In the other

$$(4) \quad r = \arctan\left(\frac{x}{F_L}\right)$$

where  $x$  is the displacement across the sensor array

As shown in Figure 3, these equations predict a variation in pitch across that face of the grating that is a parabolic curve. The parameter values used in the specific calculation were

$$\lambda = 635 \text{ nm,}$$

$$L = 100 \text{ mm,}$$

$$d = 200 \text{ mm,}$$

$$i = 88 \text{ degrees.}$$

Angle  $i$  is a grazing angle.

In equation (5) range  $D_L$  is calculated along the length of the

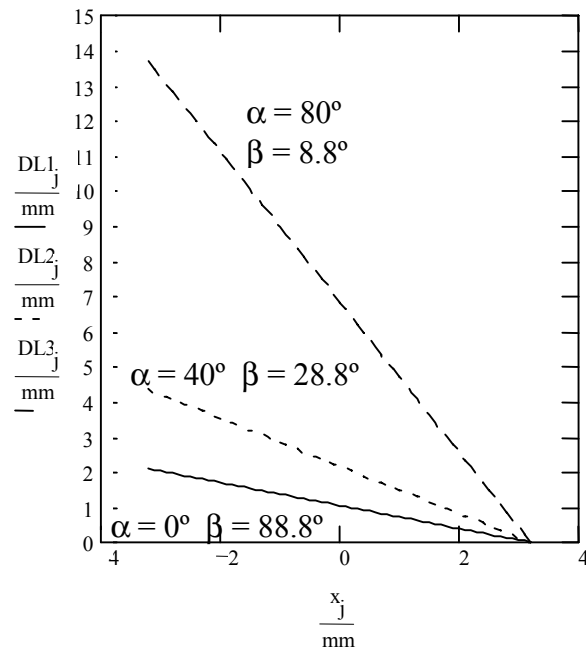


Figure 4 Range vs focal plane displacement for three angles of  $\alpha$  and their correlated occlusion liabilities  $\beta$

extreme where there is a high occlusion liability of 88.8 degrees, width to depth ratio is 50. The middle trace shows an occlusion liability of 28.8 degrees which is considered the conventional liability for most triangulation-based range finders. The ratio of width-to-depth is 20.

**Simulation**

To test our hypothesis, a grazing incidence diffraction microscope was modeled in Zemax®, a ray tracing program familiar to optical engineers. Zemax® has a feature that allows an optical element to be modeled as a holographic grating following the prescription for its creation on an optical bench. In our simulation, the hologram is positioned in the microscope as its primary objective. Zemax® allowed nine field points to be modeled. These points spanned targets over 10 cm lateral position and 1 cm of depth (10:1). The program rendered 3D layouts of the microscope as shown in Figures 5a & 5b. The image of the nine field points as seen on the focal plane array is shown in Figures 5c. Figure 5d shows the spot diagram for a typical field point that was 5 cm from the grating and displaced laterally 5 cm from centerline. The theoretical limit of resolution at the Airy disk, is indicated by the black ellipse.

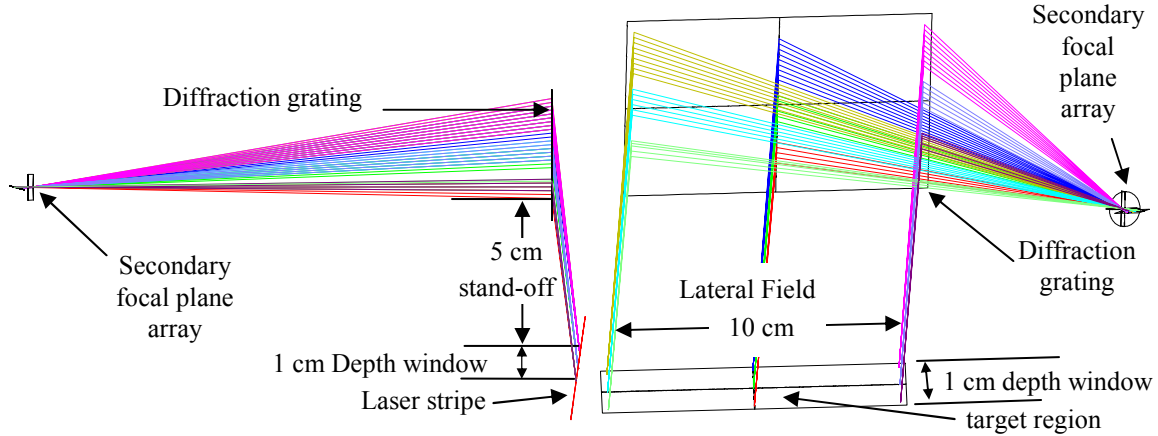


Figure 5a Zemax Model - Right view

Figure 5b Zemax Model - Isometric view

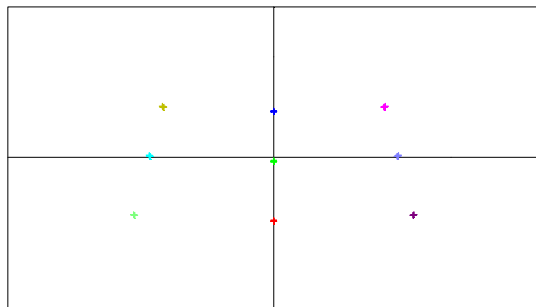


Figure 5c Image formed on 6.4 x 4 mm focal plane

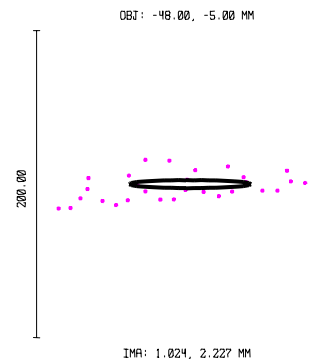
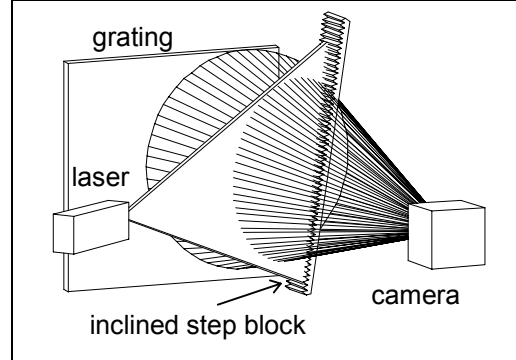
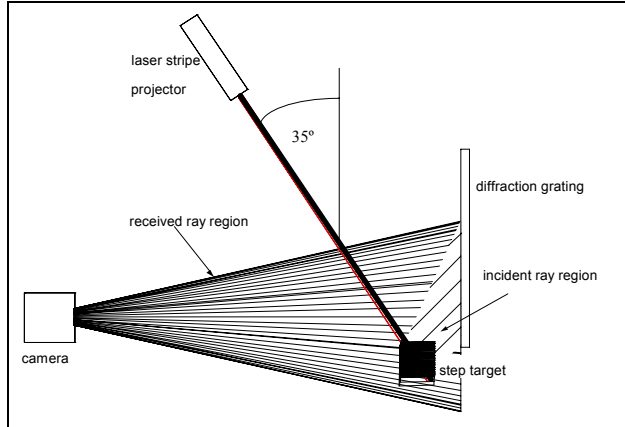


Figure 5d Spot diagram of a field point

The Zemax® simulation is a proof-of-concept. Figure 5c demonstrates that the depth-of-field is sufficient to preserve focus over the entire depth range. Figure 5c also shows that displacement on the image plane is linear with respect to distance, as proven in the P.I.’s earlier work<sup>7</sup> that led to this proposal. Lateral displacement shows artifacts of perspective foreshortening. Lateral perspective can be controlled using a proprietary secondary, not yet publicly disclosed, that counters the Scheimpflug condition<sup>8</sup> that causes it. Figure 5d shows a resolution limit close to the Airy disk. (A mathematical model for depth resolution appears in a “Theory of resolving power” section below.)

### Empirical Demonstration

We have conducted experiments with microscope optics using silver halide holograms made at incident angles of 70 degrees. Although well shy of the grazing angles possible with surface relief gratings, there is significant anamorphic magnification. In an experiment illustrated in Figures 6a & 6b, a test block was illuminated by an interrogation beam 55 degrees off the grating normal.



Figures 6a & 6b Bench setup with silver halide grating where target is a step block

inclined at 10 degrees.

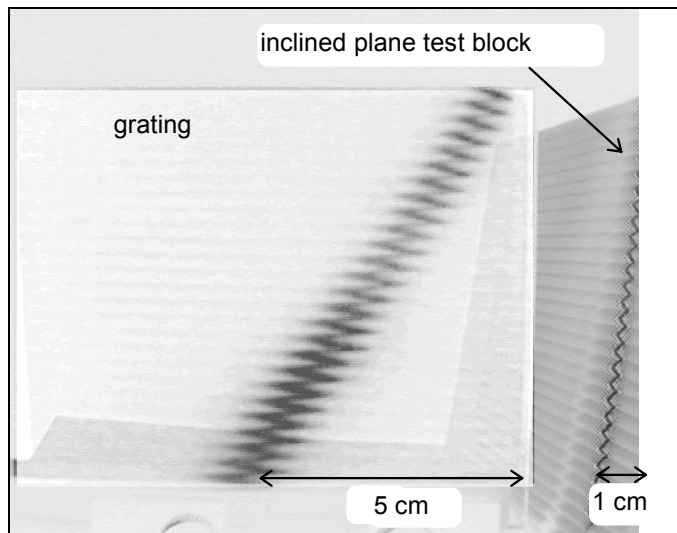


Figure 7 Focal plane image from Figure 8 bench setup  
Diffraction image to left; direct head-on view to right

The image produced by the bench setup of Figure 6 is shown in Figure 7. The step block consists of 1/10<sup>th</sup> inch uniform 90° steps and is raised to 80° relative to the base table. Note that the diffraction image of the inclined step block is five times the displacement in the range dimension when compared to the direct view, notwithstanding that the occlusion liability of the direct view has been arranged to match the occlusion liability of the diffraction image. The difference in magnification is compared using the dimension notation at the baseline of the inclined plane. Compare depth-to-height ratios between the diffraction and direct views as seen in the steps, and it is clear that the direct view is less than one, but the diffraction image shows a 5:1 ratio of depth to height.

### Surface relief grating

Unfortunately, a silver halide hologram cannot easily be used at grazing angles above 70°, because the incident radiation is reflected or transmitted largely into the zero-order rather than diffracted into higher-orders where the magnification takes place. While it is true that methods have been developed to exploit index matching between the incident wave and the hologram that could conceivably be used,<sup>18</sup> the superimposed substrates of index matching can introduce other artifacts. In fact, to date, these index matching methods are used as non-imaging optics where the grazing angle exclusively provides illuminating flux.

Fortunately, it is possible to achieve grazing incidence at angles approaching 90° by using surface relief diffraction gratings, either in reflective or transmission modes. Gratings of this type can be modeled using iterative numerical solutions for wave propagation, and one commercial software package PCGrate predicts efficiencies of up to 40% at angles of grazing incidence approaching evanescence, Figure 8. The authors of this software indicate that the predictions are unreliable at grazing angles, but one difficulty comes from predicting polarization rather than overall efficiency. Gratings with pitch lengths less than wave lengths of the incident radiation will have idiosyncratic swings in both efficiency and polarization. Typically these gratings are characterized by manufacturers empirically. Nonetheless, the basic principle upon which interference of periodic wavefronts from a grating surface form higher diffraction orders still applies, and surface relief gratings can be expected to produce a useful level of efficiency, especially given the relatively abundant flux from lasers projected down into the microscopic realm.

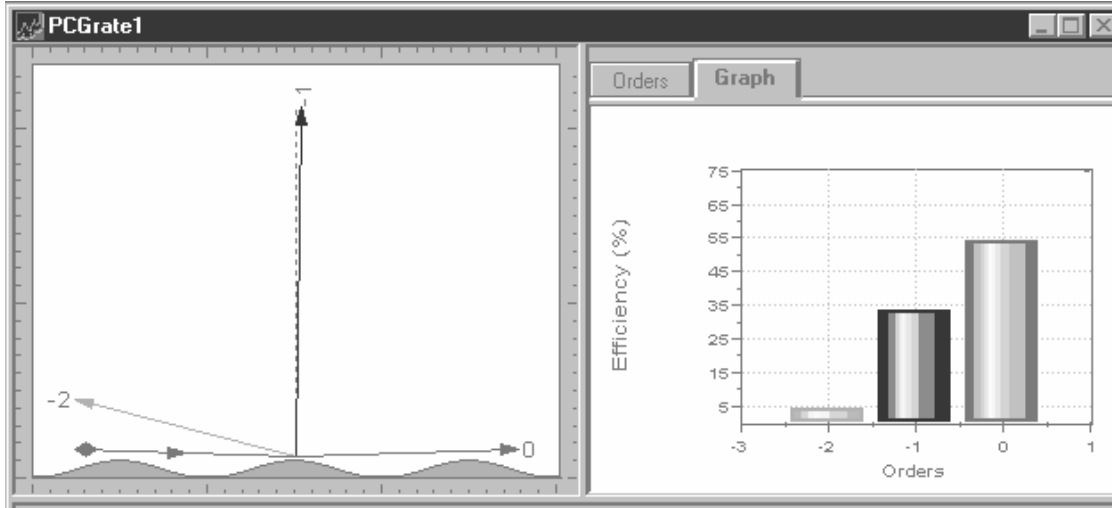


Figure 8 A prediction of PCGrate for 88° grazing incidence is a 35% efficiency in the first-order

Surface relief holograms are routinely manufactured by the display holography industry where they are used as masters for embossing. The standard spectrographic grating is also the surface relief type, often made holographically although not often with chirped frequency rules.

### Theory of resolution

Regardless of the quality and efficiency of the primary objective diffraction grating, the wave nature of light restricts its resolution to the phase interference between radiators on the incident wavefront itself. In refractive microscope optics this phenomenon is referred to as the diffraction limit. The problem has been studied with diffraction gratings where the parameter is referred to as the resolving power. Plane grating resolving power  $R$  is well understood when the object of study is separation of spectral lines.<sup>19</sup> In such studies, the resolving power is defined as the ratio of a wavelength to the smallest resolved portion of the wave length under study.  $R = \lambda / \Delta\lambda$ . The physical optics of resolving power can be simplified to the expression  $R = |nN|$  where  $N$  is the absolute number of grooves in a plane grating and  $n$  is the diffraction order. Regardless of the diffraction order, the maximum achievable spectral resolution of a plane grating is dependent upon the considerable width  $W$  of the grating in the direction perpendicular to the grooves. It is said that  $R_{MAX} = 2W / \lambda$ . This is the diffraction limit.

Resolution of a diffraction range finder can be similarly analyzed when the grating is a plane grating with regular line spacing. The distance resolving power  $R_d$  of a diffraction range finder can be predicted by correlating path lengths for the shortest discernable increments of change in distance.

$$(9) \quad R_d = DL / \Delta DL$$

Changes in path length at the grating are a caused by changes in range positions of a target as detected at some fixed wave length  $\lambda$ . The smallest resolvable shift between positions is caused by the phase shift of the measured wave length as the target changes in range. Unlike spectral resolution where changes in wave

length cause shifts in the angle of diffraction and where the width of the grating is directly proportional to the resolving power, range resolution is determined by the parameter  $p$ , the pitch of the grating. As pitch increases, resolution decreases, that is,  $R_d$  is inversely proportional to  $p$ .

Consider the generalized geometry in Figure 9. Two adjacent grating grooves of length  $p$  are shown. To observe a transition of the target from distances  $D$  to  $D'$ , a phase change must exist between the ray paths  $AB$  and  $A'B'$  sufficient to cause a perceptible extinction of a wave length  $\lambda$ . A complete extinction occurs at the half wave length, so for a resolvable increment of range  $\Delta D$  it can be argued that

$$(10) \quad A + B = A' + B' - \frac{\lambda}{2}$$

$\Delta D$  itself is the difference between  $D'$  and  $D$  at the offset of  $2p$ . In other words:

$$(11) \quad \Delta D = 2p + D' - D$$

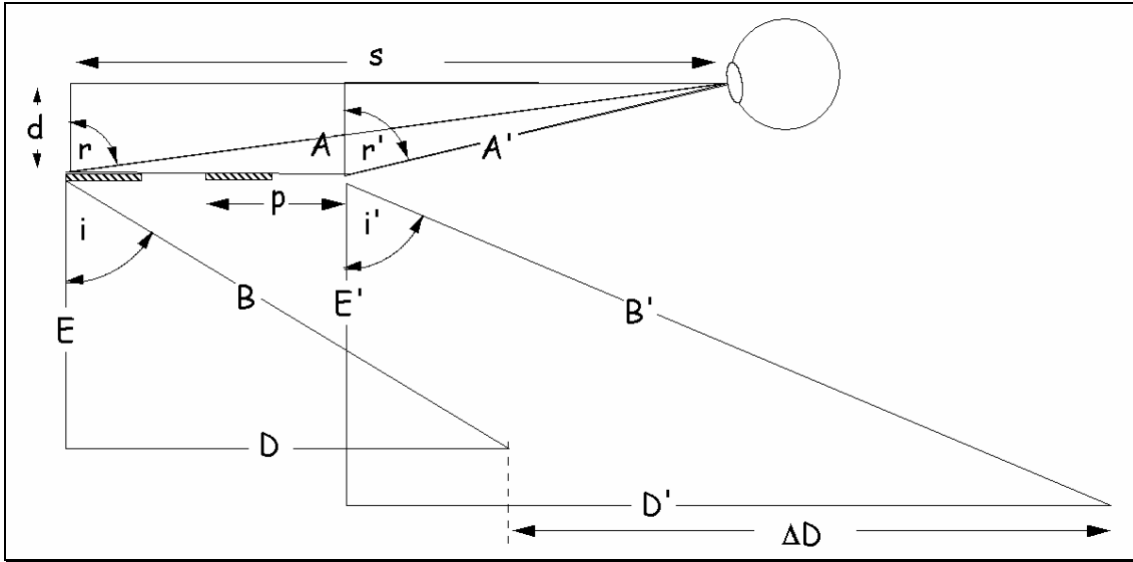


Figure 9 Generalized model for diffraction range finder resolution calculation

To match the grating for the distances being ranged, legs  $D$  and  $E$  can be entered into the Diffraction Equation along with parameters  $s$  and  $d$  for the location of the sensor to specify the pitch  $p$ . (Note that the order  $n = 1$  is being used, so this term is not needed in Equation (13) and will be dropped from subsequent expressions).

$$(12) \quad r = \arctan\left(\frac{s}{d}\right)$$

$$(13) \quad p = \frac{n\lambda}{\sin(i) + \sin(r)}$$

According to the geometry of Figure 9 these identities also apply:

$$(14a) \quad A = \frac{d}{\cos(r)} \quad (14b) \quad B = \frac{D}{\sin(i)}$$

The triangle  $B'D'E'$  must be calculated. To do this we determine angle  $i'$  which is dependent upon  $r'$  by virtue of the Diffraction Equation where  $\sin(r') + \sin(i') = \lambda / p$ .

First:

$$(15) \quad r' = \arctan\left(\frac{s - 2p}{d}\right)$$

Then:

$$(16) \quad i' = \arcsin\left(\frac{\lambda}{p} - \sin(r')\right)$$

As per Equation (10) we can say:

$$(17) \quad B' = A - A' + B + \frac{\lambda}{2}$$

where

$$(18) \quad A' = \frac{d}{\cos(r')}$$

$$(19) \quad D' = B' \sin(i')$$

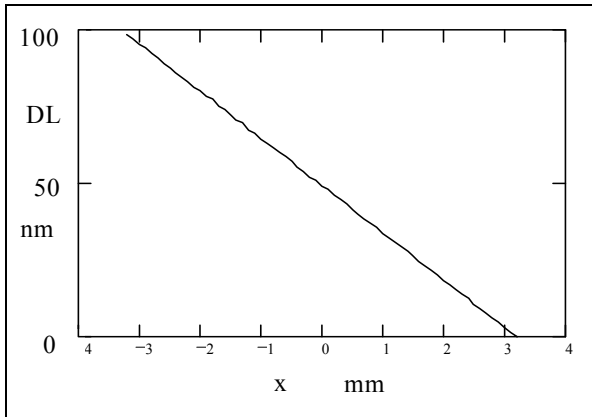


Figure 10 A prediction ignoring the wave nature of light. Range in nm vs. focal plane displacement in mm

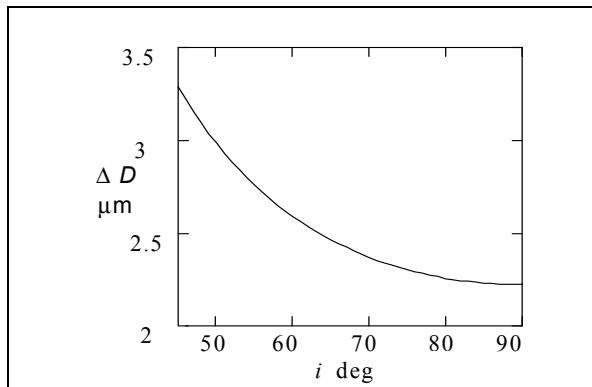


Figure 11 A prediction using our resolving power model Resolution vs. angle of incidence for targets at 10 cm

The procedure for calculating the resolution limit of a diffraction grating primary objective calibrates the potential for 3D range acquisition far better than the simple geometric optics of grazing incidence derived in equations (1-8). Those equations can produce erroneous predictions. For example, if the grazing angle is set to 89.99999 degrees and the interrogation angle  $\alpha$  of a 635 nm laser is 79.8 degrees, equations (1-8) predict that a 10 cm grating can produce a profile that is 100 nm in range using a camera with a 6.4 mm focal plane (Figure 10). This would suggest a magnification of 100,000 times, an exaggerated figure that simply is not possible in the real world due to the wave nature of light.

A sample calculation using the definition of  $\Delta D$  from equations (9-19) shows that the shortest distance that can be resolved decreases to a limit as the angle of incidence approaches 90 degrees. Given a baseline of 10 cm from target to grating where the wave length is 635 nm, the resolution at the center of the grating could vary from 3.5 to 2.2225 microns as the incidence angle varied from 45 degrees to 90 degrees (see Figure 11).

Compared to a conventional microscope, a resolution of 2.6 microns at 635 nm is greater than the comparable diffraction limit for refraction objectives in 2D, but such objectives must be refocused for each 3D plane. Moreover,

the diffraction limit goes up as the stand-off increases. This is why conventional microscope objectives have a planar face on the specimen side and why their highest magnification is achieved at the shortest stand-off.

There are many other ways of using the same set of equations for evaluation and optimization. For example, it can be shown that with a grating stand-off of 1 cm, the theoretical range resolution drops to 1.65 microns for light of wave length 635 nm. It is self-evident that the resolution can be improved by the use of shorter wave lengths, as is now possible with the new generation of blue and ultra violet laser diodes. Interestingly, the resolution remains quite good at very great distances from the grating. For example, the model predicts 6 mm resolution at 1 km with a large grating. As with all new technologies, there is always the possibility of encountering some unexpected predictions that suggest novel applications.

In order to fully examine the potential of grazing incidence diffraction range finders in either their microscopic or telescopic regimes, it would be prudent to refine the resolution model. When the primary objective is fabricated using holography, the performance of the resulting optical system is affected by diffraction found on the bench optics that make the grating. These parameters can be entered in the Zemax-E program which generates a mathematical model of a diffraction grating using key parameters from the bench including the size of the pin hole of the spatial filter and its associated refractive optics.

Of course, the empirical data must be acquired and processed. The diffraction limit is not the statistical limit of the resolution, since the receiving camera will have multiple photosites illuminated by the higher-order flux. The spatial energy on these sites is distributed in a Gaussian bell curve that can be converted into an intra-pixel position estimate. In most cases, such estimates increase the effective resolution of the range finder by a factor of 4. As a practical matter, we expect sub micron resolution in 635 nm illumination. Dr. Douglas Lyon, joint-inventor of the chirp grating for a diffraction range finder, is the author of two textbooks on Image Processing<sup>20</sup> and has modeled the extraction of such centroids.

### Commercial Potential

Sales of all microscopes in year 2000 have been reported as \$800 million in a marketplace that is dominated by visible light types.<sup>21</sup> Of this market, a microscope that would directly compete with a diffraction range finder type is the 3D confocal type which was reported to have had a worldwide market in 2000 of \$55 million or six per cent of the total market. Its market share continues to grow, and by 2001 confocal sales were reported to be 7.5% of the total world market.<sup>22</sup> In their issue on Industrial Microscopy the trade publication *Photonics Spectra* asserts "It's a three-dimensional world for industrial microscopy these days."<sup>23</sup> Their special issue is devoted to microscopes used in what is called "microsurface mapping." Confocal and interferometric microscopes are prominently featured.

Confocal instruments are based on properties of refraction which are exploited to detect very small resolved points in all three dimensions. Working within sub millimeter distances to the target, the confocal objective can resolve sub-micron diameters in visible light. The trade-off is that there is little stand-off from the specimen, and the (x,y) to z ratio is 1:1:1. In order for areas to be scanned, the source illumination, typically a laser, must be scanned in two dimensions over the field-of-view of the primary, typically millimeter diameters. For larger work areas the specimen stage must be moved rapidly and accurately over the acquired distances. Biologists can live with these restrictions when specimen slides hold micron scale objects, but confocal microscope specifications do not work well in industrial metrology settings where surfaces tend to be large and stand-off to target must be maximized.

Another 3D microscope technology used in industrial inspection is based on interferometry. Here long stand-off can be achieved with instantaneous acquisition of wide fields-of-view at nanometer resolution. Unfortunately, the method is restricted to contiguous surfaces where continuity is measured in the same units as the device's very high resolving power. Interferometers are capable of relative distance measurement as opposed to absolute measurement where the output is in universal co-ordinates. Given the local co-ordinate base of the interferometric image, discontinuities go undetected without taking so many additional exposures that the method is impractical in almost all industrial metrology settings. Also, it is important to note that the very high level of precision required for their construction results in high cost.

Our patented diffraction range finding method takes readings in absolute units of distance and does not suffer from the ambiguities of a relative co-ordinate base as do interferometric microscopes. Compared to the confocal method, the diffraction range finder has the capability of long-standoff to target, very high width to depth ratios, and instantaneous profile acquisition, as opposed to point by point acquisition.

Competitive standing in the field of 3D microscopy is advanced by innovation and patent protection. A study made public by the UK Competition Commission, a British government research group that evaluates how to protect proprietary technologies. "There is steady demand for improvements in advanced 3D microscopy to enable new applications... It has been put to us, both by customers and by suppliers, that the market for such systems (as distinct from classical microscopes) is growing. The relevant markets are characterized by effective competition, within the limits set by patent protection." The Competition Commission further states, "In considering competition within the relevant markets, we conclude that they are characterized by high product differentiation, with competition depending largely on product features rather than directly on price. We observe that innovation is crucial in providing a competitive advantage."<sup>24</sup>

There are many factors that will determine the success of the commercialization of 3D microscopes. Our method fully meets two of these. Firstly, the technology is innovative. There are no microscopes which use holographically fabricated diffraction gratings as their primary objective elements. Secondly, we hold the patent for the method. The patent is in force in the US and throughout the EPO. It is under Examination in Canada and Japan where there is a reasonable expectation of adoption.

Unique specifications of the technology additionally lend credence to its potential commercial worth. Any 3D camera can replace all 2D cameras if the 2D data is equivalent, but a 2D camera does not function as a 3D camera. This is a distinction similar to the emergence of color film as the default in photography. As the expert said about the microscope marketplace, "It is a three-dimensional world..."

Of course, when there is a price penalty for the third dimension and two-dimensions will do, then the default may not be 3D. However, there is a feature of holographic surface relief diffraction gratings that will play a significant role in cost reduction, notably, diffraction grating microstructures can be replicated in plastic by embossing methods. Any CD or DVD will serve as an object example of this fact. The nickel plated holographic master may cost tens of thousands of dollars to fabricate, but once an embossing master exists, duplicates of nearly equivalent quality are practically free.

Inexpensive primary objectives for microscopes would alter the performance specifications of industrial metrology instruments, because the exposed optic of the instrument could be replaced easily. This opens the marketplace to many *in situ* applications where expensive refractive microscope objectives would be at risk. From a profit stand point, the patent holder could not do better than to have "throw away" front-end optics. Patent protection for the technology would not only apply to the capital instrument but also to the consumables. Elements costing little to manufacture would be sold at substantial profit, even when the cost to the consumer was very low when contrasted with the competition from refractive microscopes.

An inspection microscope manufacturer, Aspex, Inc., has taken a financial interest in the patent in order to originate a version of their inspection microscope, the Spinktrak<sup>®</sup>, using the technology. Aspex is a small company that enjoys deep penetration into a niche microscope market, spinnerette inspection. Aspex can immediately exploit the 3D microscopy technology in this niche where about 20% of its customers have already requested the 3D capabilities that come from the proposed instrument. In particular, there are spinnerettes that cannot be imaged by conventional microscopy, because they are on spherical substrates. These "dome" spinnerettes have extremely fine and dense hole networks that are not candidates for the existing SpinTrak<sup>®</sup> 2D microscopes with their image processing algorithms. The introduction of a new version of the SpinTrak<sup>®</sup> with the 3D microscope would be assured of sales in six figures within two years of introduction.

Aspex will also take the 3D SpinTrak<sup>®</sup> into the general marketplace if the technology is successful. Aspex will be in a position to negotiate manufacturing licenses or to manufacture the product in their own plants. If consumable supplies become a commodity, then this business model will apply, that is, an inventory of every type of consumable will be made available through catalog sales. The hardware marketplace could reach into the tens of millions of dollars if current market size is a guide. Aspex has had gross sales of \$9.7 million for their inspection microscope alone. However, hardware sales profit margins will be constrained by the expense of manufacture. The secondary marketplace of consumables may not be nearly as large, but profit margins can be very high. This is because the technology is patent-protected in US, Canada, Europe and Japan, and the actual cost per part promises to be very low after the initial start-up charges.

## Conclusion

Holographic microscopy, envisioned by Dennis Gabor in 1948 but never realized in practice, has a practical implementation using a point source hologram, a chirped frequency diffraction grating, as a microscope primary objective. The hologram is fabricated as a surface relief micro-structure and is positioned at an angle of grazing incidence to form a profile of a topological target under monochromatic stripe illumination. This recently patented method can provide rapid and accurate acquisition of 3D surface profiles in absolute units of distance. The method also promises improved depth-of-field, width-to-depth ratio and stand-off-to-target when compared to conventional microscopy based on refractive primary objectives. The new method can be implemented with replicated gratings, suggesting that the microscope primary objective would be a consumable component suitable for use in hostile environments. A proof-of-concept is contemplated under Phase I SBIR funding from the National Science Foundation.

## References

---

- <sup>1</sup> D. Gabor, "Microscopy by reconstructed wavefronts," Proceedings of the Royal Society of London, Vol. 197, pp. 454-487, (1949).
- <sup>2</sup> Collier, Burckhardt & Lin, *Optical Holography*, Academic Press, 1971, p 360 ff
- <sup>3</sup> Thomas DeWitt, Range Finding by Diffraction, U.S. Patent 4,678,324, July 7, 1987
- <sup>4</sup> Thomas DeWitt, Range Finding by Diffraction, England (0,343,158), France (87901777.0), Germany (P3789901.5), Sweden (87901777.0), Switzerland (CH675299) and Japan (JP2502398T)
- <sup>5</sup> DMI-9420321 A Hand-Held Three Dimensional Scanner
- <sup>6</sup> *NASA Tech Briefs*, Technology 2007, "Small Business Stars", December 1997, Vol. 21 No. 12, p. 32
- <sup>7</sup> Tom Ditto and Douglas A. Lyon, "Moly a prototype handheld three-dimensional digitizer with diffraction optics," *Optical Engineering*, January 2000, Vol 39 No. 1, pp. 68-78
- <sup>8</sup> Thomas D. Ditto and Douglas A. Lyon, "Variable grating for diffraction range finder", US Patent 6,490,028, Dec. 3, 2002
- <sup>9</sup> DE69723110D, DE69723110T, EP0963541 (WO9944013), ES2196397T
- <sup>10</sup> CA2277211
- <sup>11</sup> JP2001513899T
- <sup>12</sup> Thomas Ditto, "Kilometer scale primary objective telescope with no moving parts," *Large Ground-based Telescopes*, Proceedings of SPIE Volume: 4837, Feb. 2003, pp. 649-658
- <sup>13</sup> T.D. Ditto, "Three-dimensional microscopy using a diffraction grating primary objective," *Biophotonics*, Proc. SPIE Vol. 5578, p. 167-178
- <sup>14</sup> Christopher Palmer, *Diffraction Grating Handbook*, 2<sup>nd</sup> Edition, Milton Roy Company, 1994, p.9
- <sup>15</sup> [http://www.drillamerica.com/PDF/plate\\_calc.pdf](http://www.drillamerica.com/PDF/plate_calc.pdf) shows the calculation for the grazing exodus case
- <sup>16</sup> [http://www.optometrics.com/prod/fr\\_spectro.html](http://www.optometrics.com/prod/fr_spectro.html)
- <sup>17</sup> Francis S. Luecke, "Tuning System for External Cavity Diode Laser," US Patent 5,319,668, (June 7, 1994)
- <sup>18</sup> Nicholas J. Phillips et al, "Grazing incidence holograms and system and method for producing the same," U.S. Patent No. 5,822,089, October 13, 1998
- <sup>19</sup> Christopher Palmer, *Op. Cit.*, p.7
- <sup>20</sup> Douglas Lyon, *Image Processing in Java*, Prentice Hall, 1999
- <sup>21</sup> "3D Pathology" [3d-pathology.preme.de/downloads/dup-public.pdf](http://3d-pathology.preme.de/downloads/dup-public.pdf), p. 10
- <sup>22</sup> <http://www.the-infoshop.com/pdf/tk12574.pdf> p. 5
- <sup>23</sup> Paula M. Powell, "Industrial Microscopy Gets Down to Work," *Photonics Spectra*, August 2004, Vol. 38, No. 8, p. 58
- <sup>24</sup> [http://www.competition-commission.org.uk/rep\\_pub/reports/2004/488zeiss.htm](http://www.competition-commission.org.uk/rep_pub/reports/2004/488zeiss.htm)